Full-volume investigation of moving rigid and flexible wings using Lagrangian Particle Tracking of surface markers and tracer particles

D. Schanz, R. Konrath, R. Geisler, A. O. Erdogdu, J. Agocs, A. Schröder
Institute of Aerodynamics and Flow Technology, German Aerospace Center (DLR), Göttingen, Germany
* Correspondent author: daniel.schanz@dlr.de

Keywords: Lagrangian Particle Tracking, Shake-The-Box, Iterative Particle Reconstruction, Triangulation, Bird flight, Bio inspired flight

ABSTRACT

This work describes a combined measurement of the volumetric flow around moving wings and the shape and orientation of the rigid or flexible wing surface. For both, the Shake-The-Box Lagrangian Particle Tracking method is applied, tracking polyamide seeding particles in the water flow, as well as a high number of surface markers on both sides of the wing. A system of eight high-speed cameras is used in order to capture the full volume from all sides, yielding long time-resolved sequences of approx. 6 seconds length.

The aim is to simultaneously determine the aerodynamic and the structural forces, thereby solving the so-called Collar's triangle. The movement patterns of the investigated wings are inspired by flapping wing flight of birds. This measurement shall supply data for the development of advanced Micro Aerial Vehicles, capable of flying efficiently and with a high resistance to external disturbances.

1. Introduction

The investigation of the flapping flight observable in nature on flying birds and insects is of high interest for developing Micro Aerial Vehicles (MAVs) operating in the low Reynolds number regime, since the performance of conventional aircraft designs deteriorates rapidly as the Reynolds number decreases below 10^5 (Mueller and DeLaurier, 2003). The goal of biology-inspired flapping wing mechanisms is not only to generate lift and thrust in a more efficient way (Jones and Platzer 2015) for longer flight endurances, but also to achieve a high degree of agility of the vehicle, for example, when encountering unpredictable wind gusts (Mohamed et al., 2021). Flapping wings can generate unsteady three-dimensional flow structures changing the pressure distribution on the wing which are sensitive against the wing kinematics and flow parameters. An insect, for example, can produce additional lift by generating a large leading-edge vortex inducing an additional suction peak on the wing surface (Lehmann, 2004). Furthermore, structural wing flexibility can be an important aspect of wing designs, for example, to improve thrust efficiency (Shyy et al., 2010)

For an aerodynamic analysis of the underlying flow phenomena and aeroelastic effects of flapping wing configurations, developments on non-intrusive optical measurement methods play an important role in order to get three-dimensional data of the unsteady flow fields (Ehlers et al., 2016) as well as of wing motions and shape deformations (Wolf and Konrath, 2015). Direct measurements of the loads as thrust and lift on flapping wing configurations are often difficult, because of lightweight wings and the very small forces involved. However, under certain conditions, the data of combined velocity field and surface deformation measurements can be used to determine the aerodynamic and the structural forces, comprising the inertia and elastic forces, the so-called Collar's triangle (González Saiz et al., 2021). This seems to be a promising approach especially in combination of state-of-the-art Lagrangian particle tracking methods (Schanz et al., 2013, 2016, 2021) for time-resolved and volumetric flow field measurements. The high precision and spatial resolution allow for calculations of the related pressure fields (Gesemann et al., 2016) which can be used to estimate the aerodynamic forces if the friction forces can be assumed to be small.

In the present paper, a method is described to use the Shake-The-Box (STB) method to measure both the flow field and the shape of moving surfaces in the flow with high spatial resolutions. First results of a measurement conducted in a water tunnel on different flapping wing configurations are presented to show the performance of the technique in view of solving the Collar's triangle by further data processing.

2. Test facility and measurement setup

A dynamic test rig based on a hypocycloid gear (Huhn, 2015) has been designed at DLR for underwater flapping wing applications (see Figure 1 a and b). Three NACA0012 wings with different flexibility, to be attached to the end plate, have been constructed (half span: 150 mm, chord: 50 mm). The wings perform a two-dimensional motion, i.e. within the x,z-plane, whereas the pitch axis is constantly pointing in the y-direction. Markers with approx. 0.5 mm diameter were printed onto the wings with pseudo-random distribution to allow detection of the wing motion and deformation (see Figure 1 c and d).

The dynamic test rig was installed in the closed-circuit water tunnel at the Aerodynamic Institute (AIA) of the RWTH-Aachen tunnel to investigate the instantaneous aerodynamics of flapping wings (see Figure 1 f and g). The facility provides a 1.5 m wide and 1 m high test section and was operated at a free stream velocity of U = 0.44 m/s. Various pitching and plunging motions at a frequency of 1.03 Hz were realized for all three wings, both with and without water flow.

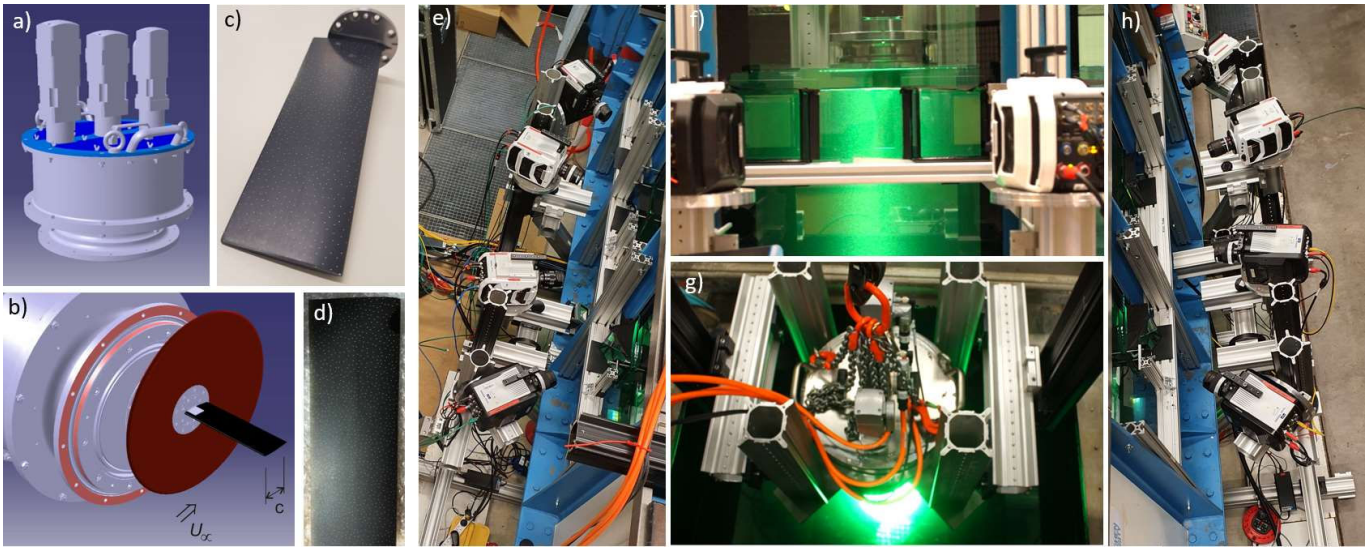

Figure 1: a) DLR dynamic test rig with three synchronized servo motors and gear box; b) half wing installed on end plate; c) rigid wing; d) flexible wing; e) and h) 4 cameras installed on each side of the wind tunnel, forming a common camera system; f) side view of illuminated wing and particles; g) dynamic test rig installed on the top of the water tunnel

3. Data evaluation and results

A system of eight high-speed cameras (Phantom V2640 and V1840) were installed in two groups at both sides of the tunnel, providing a full view around the moving wing (see Figure 1 e and h). Illumination was realized using three high-power LED arrays, collimated by a 1000mm lens and located beneath the tunnel. This way, a circular light volume with approx. 20 cm diameter was created, which was completely seen by all cameras (apart from the regions blocked by the wing for each camera). The wall-normal extent is approx. 220 mm. The water was seeded using 60 µm polyamide particles. The cameras and LEDs were operated at 2 kHz repetition rate, yielding sequences of 12597 images at the full camera resolution of 4 MP.

The cameras were calibrated using a 3D calibration target, which was translated by 150 mm in spanwise direction. Volume-self-calibration (Wieneke 2007) and OTF calibration (Schanz et al. 2013) were applied. Figure 3(a) shows the positions of the cameras as given by the calibration in relation to the common volume, seen from above.

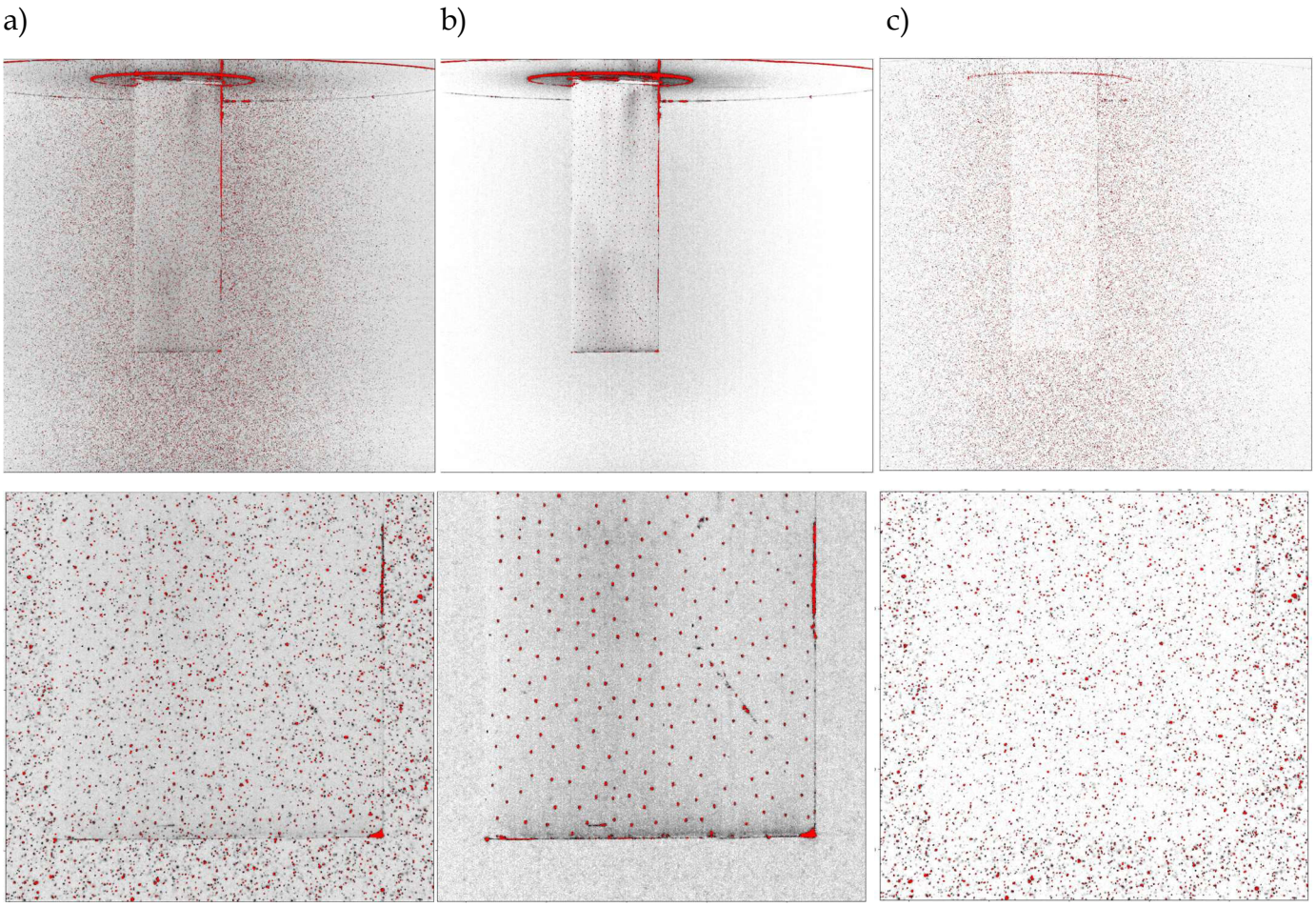

Figure 2: Full view (top row) and exceprt (bottom row) from camera image. a) raw image; b) minimum over six images, extracted at the same phase position of the wing movement; c) minimum image subtracted from camera image (c=a-b)

Both the particles, as well as the markers on the wing have been captured within the same images. The aim is to separately track both kinds of 3D points all around the model via Lagrangian particle tracking using the Shake-The-Box (STB) method (Schanz et al. 2016).

Evaluation starts with the detection of the wing. As multiple cycles of the wing movement were captured in each run, a separation of the wing markers from the particle images is possible via the minimum images of the captured six instances of each phase. Figure 2 a and b show an exemple for a raw camera image from a single camera and a phase-resolved minimum image. The tracking of the wing markers is then performed using STB on these minimum images, available for one full cycle (1940 images).

Figure 3 b shows tracked markers on a rigid wing, viewed from above for several phases of a motion inspired by hummingbird-flight (Nabawy, Crowther, 2015) (without inflow). A quick rotation of approx. 160 degree is followed by smaller-scale oscillations, while the wing is

performing a plunging motion with 100 mm amplitude. Due to the difficult viewing conditions (in certain positions of the wing, many marker points are only visible in one or two cameras, due to geometry and reflections), not all markers can be tracked over the whole cycle. However, the total number of captured markers (600 - 800) is always enough to allow for a reliable detection of the wing. Figure 3 c shows a side view of the wing markers for one time-step at the time of the rotation movement.

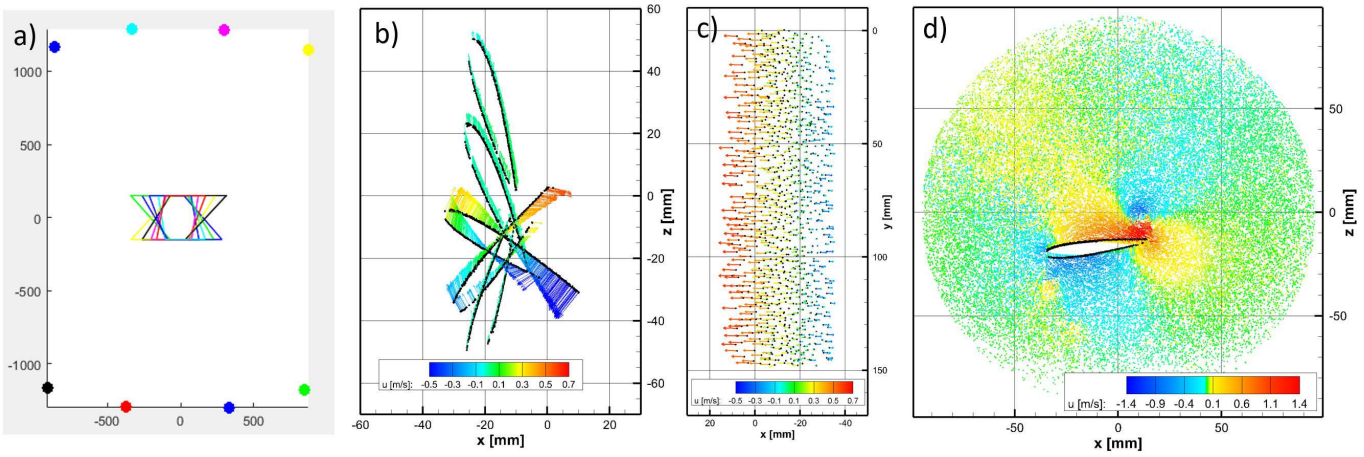

Figure 3: a) The calibrated camera setup, viewed from above. The camera lines-of-sight describe the commonly imaged volume; b) tracked wing markers with velocity vectors at four different phases of a combined ptiching and plunging movement, inspired by hummingbird flight (viewed from above) ; c) side view of one phase of b); d) tracked particles at one time-step of the same hummingbird-inspired movement, viewed from above (without flow of the tunnel). Tracked wing markers given as black dots.

The particle tracers are identified in a second process. The same time-resolved minimum images that were created for the tracking of the wing markers are subtracted from the original camera images in order to remove the marker images and most of the strong reflections on the end plate. See Figure 2 c for an example. The resulting images are used to reconstruct 3D positions using advance IPR processing (Wieneke 2013, Jahn et al. 2021). For the cases without water flow, Variable-Timestep STB processing (VT-STB, Schanz et al. 2021) was applied due to the high dynamic velocity range. Time-separations of Δ_S = 10, Δ_S = 4 and Δ_S = 2 were used for a three-pass reconstruction. Approximately 100.000 particles are tracked after the final iteration. Figure 3 d shows an exemplary result from a single time-step of the same case as above. The particles are given as small circles with a velocity vector, color-coded with streamwise velocity (though no flow is present here), while the wing markers are depicted as black circles with velocity vectors, also color-coded with streamwise velocity. The quick rotational movement of the wing induces strong vortices in the fluid, where velocity magnitudes up to 1.5 m/s are reached.

Applying regularized interpolations by fitting the parameters of a system of cubic B-splines to the tracked particles of each time-steps (FlowFit data assimilation, Gesemann et al. 2016) yields a continuous function of velocity, acceleration and pressure, allowing a continuous sampling of the velocity-gradient-tensor. Figure 4 shows results for three consecutive phase positions, starting with a time, where the wing is performing the quick rotation. The creation of a strong vortices at the trailing edge and a weaker one at the leading edge can be witnessed. Finishing the rotation, the wing flings away the trailing edge vortex, that forms an L-shape together with the vortex created at the wing tip.

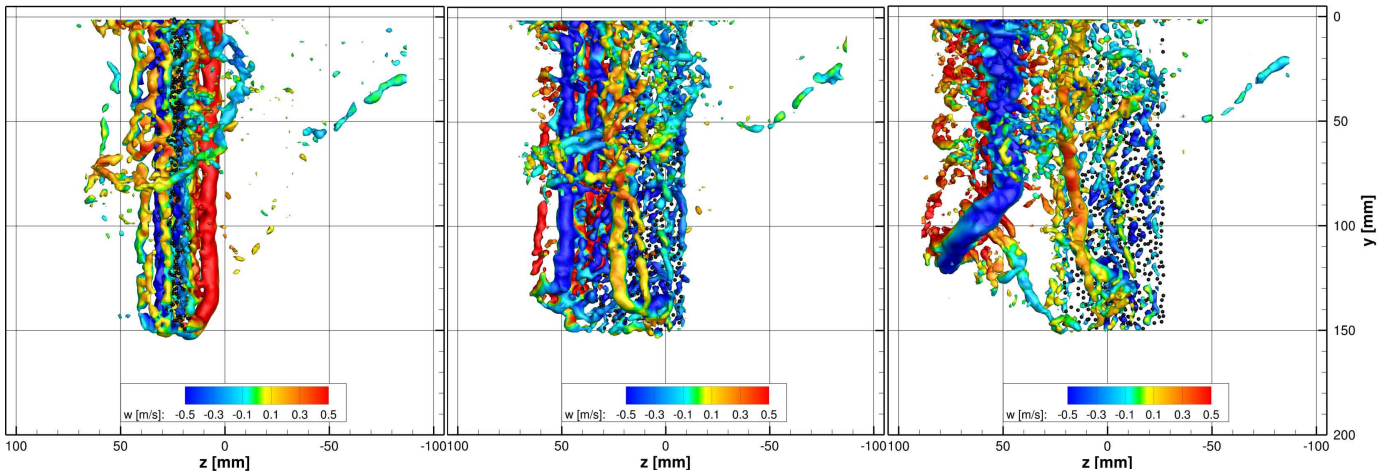

Figure 4: Instantaneous flow structures (isosurfaces of Q-criterion) of three phases, each separated by 60 m***s***, gained by FlowFit interpolations of the tracks from a case with hummingbird-flight inspired wing motion (see Figure 3). Tracked wing-markers shown as black spheres.

For cases with water flow, two-pass VT-STB evaluations with Δ_S = 4, and Δ_S = 2 were conducted. Figure 5 shows instantaneous results for an exemplary case with a free stream velocity of U = 0.44 m/s and a wing stroke that was inspired by owl flight (Wolf and Konrath 2015). Due to the slower movement of the wing, the velocity magnitudes are lower compared to the previous case, reaching up to 0.7 m/s close to the leading edge. Flow separation can be seen on the side that is opposite to the direction of wing movement.

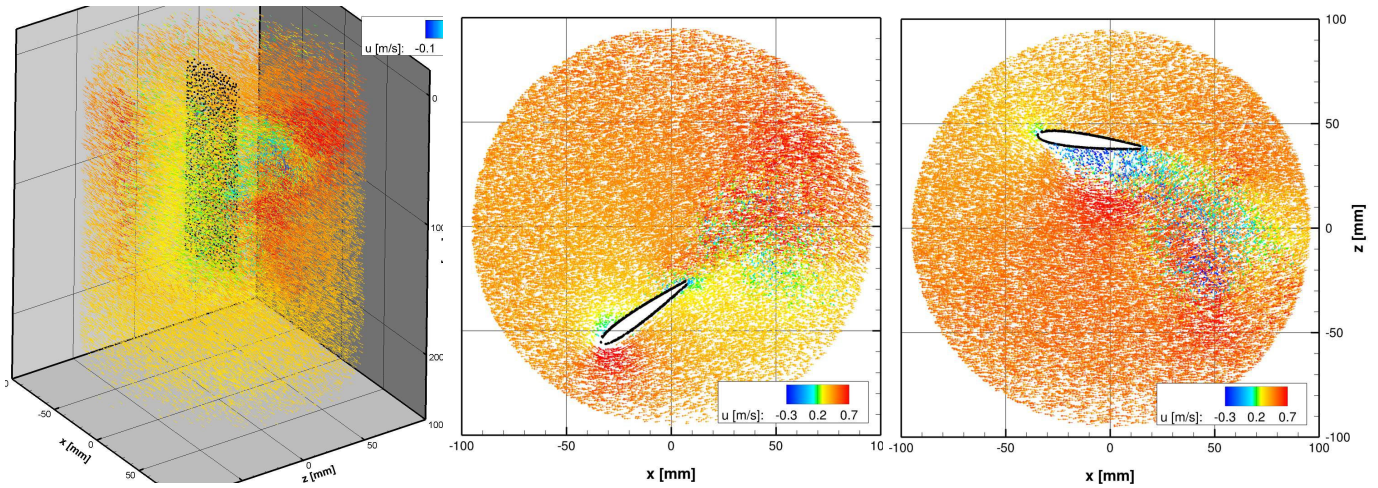

Figure 5: Instantaneous tracking results from a case with owl-flight inspired wing motion and a free-stream velocity of U = 0.44 m/s. a) 3D view of the full volume; b) and c) top view of a 125 mm deep cut at two phase positions. Wing markers given as black dots.

FlowFit interpolations (see Figure 6) were used to identify flow-structures in the same dataset. The wing tip vortex is clearly visible in the first two images. A system of vortices develops in the separated region, which detaches and transitions into smaller vortical structures. When doing so, the main structure is vertically folded up, as it is being transported downstream. This process can also be witnessed in the 3D pressure field (see Figure 7, displaying isosurfaces of the normalized pressure $\bar{p} = p/\rho$), where the separation region shows up as an extended low-pressure zone, attached to the wing, which eventually detaches and is folded up before breaking up in smaller structures while convecting downstream.

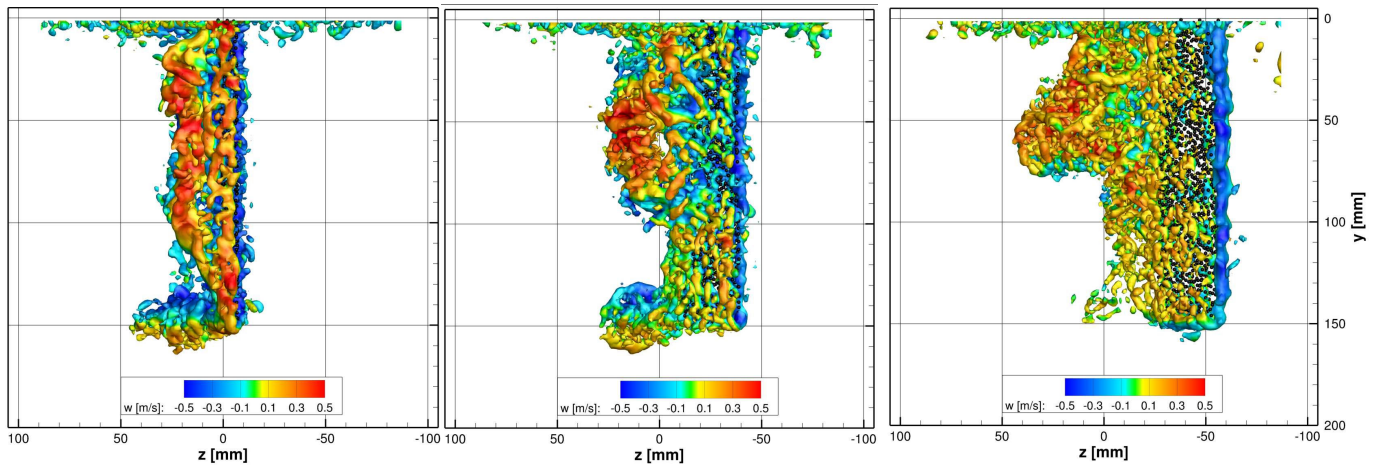

Figure 6: Instantaneous flow structures (isosurfaces of Q-criterion), gained by FlowFit interpolations of the tracks from a case with owl-flight inspired wing motion and a free-stream velocity of U = 0.44 m/s (see Figure 5).). Tracked wing-markers shown as black spheres.

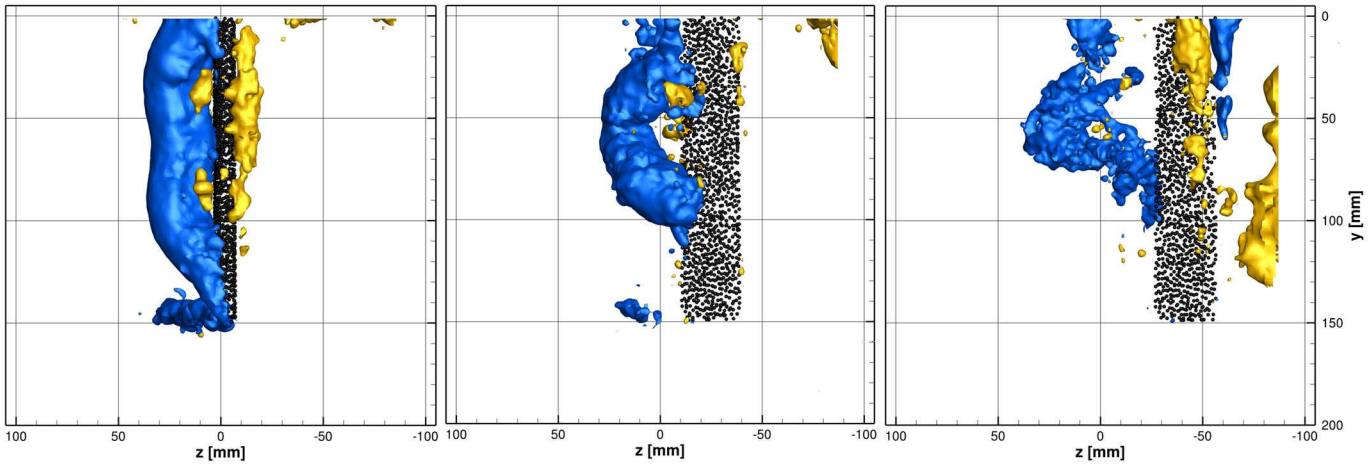

Figure 7: 3D pressure fields as isosurfaces at $\bar{p} = 0.05\ m^2/s^2$ (yellow) and $\bar{p} = -0.1\ m^2/s^2$ (blue), given by FlowFit interpolation, for the same time-instants as shown in Figure 6.). Tracked wing-markers shown as black spheres.

Outlook

The evaluation is ongoing. The next task will be to fit a 3D FE-Model of the wing to the captured marker cloud, in order to fully describe the flexing of the wing. The fitted model will then be used in the FlowFit data assimilation method (Gesemann et al. 2016) as a boundary condition, in order to extract (surface) pressure and load distributions. Advances of the tracking process will be included, e.g. 3D-masks will inform the reconstruction methods, which regions in space are blocked by the presence of the wing for each camera.

Acknowledgements

This project has received funding from the European Union's Horizon 2020 research and innovation programme under grant agreement No 769237 HOMER and by the Deutsche Forschungsgemeinschaft (DFG) through Grant No. SCHR 1165/5-1/2 as part of the Priority Programme on Turbulent Superstructures (DFG SPP 1881).

References

Ehlers, H., Konrath, R., Wokoeck, R. and Radespiel, R. (2016). Three-Dimensional Flow Field Investigations of Flapping Wing Aerodynamics. AIAA Journal 54 (11):1-16.

Gesemann, S., Huhn, F., Schanz, D., Schröder, A. (2016). From noisy particle tracks to velocity, acceleration and pressure fields using B-splines and penalties. 18th Int. Symp. on Appl. of Laser and Imaging Tech. to Fluid Mech. Lisbon, Portugal, July 4 – 7.

González Saiz, G., Sciacchitano, A., Scarano, F. (2021) Towards the closure of Collar's triangle by optical diagnostics. 14th International Symposium on Particle Image Velocimetry – ISPIV 2021, August 1–5.

Huhn, F. (2015). Getriebe für eine Auftriebsfläche, Schlagantrieb und Unterwasser- oder Luftfahrzeug, DE 10 2015 121 995, Deutsches Patent- und Markenamt.

Jahn, T., Schanz, D., Schröder, A., (2021) Advanced iterative particle reconstruction for Lagrangian particle tracking. Exp Fluids 62, 179.

Jones, K.D., Platzer, M.F. (2015) Flapping-Wing Propelled Micro Air Vehicles. In: Valavanis K., Vachtsevanos G. (eds) Handbook of Unmanned Aerial Vehicles. Springer, Dordrecht.

Lehmann, F. O. (2004). The mechanisms of lift enhancement in insect flight. Naturwissenschaften 91(3): 101–122,

Mohamed, A., Watkins, S. and. Jones, A.R. (2021) Flight-Relevant Gusts: Computation Derived Guidelines for Micro Air Vehicle Ground Test Unsteady Aerodynamics, Journal of Aircraft 58 (3).

Mueller, T. J., DeLaurier, J. D. (2003). Aerodynamics of Small Vehicles, Annual Review of Fluid Mechanics, Vol. 35, pp. 89–111.

Nabawy, M. R. A., Crowther, W. J. (2015). Aero-optimum hovering kinematics. Bioinspir. Biomim. 10 044002

Schanz, D., Gesemann, S., Schröder, A., Wieneke, B., Novara, M. (2013) Non-uniform optical transfer functions in particle imaging: calibration and application to tomographic reconstruction. Meas Sci Technol 24:024009.

Schanz, D., Gesemann, S., Schröder, A. (2016). Shake-The-Box: Lagrangian particle tracking at high particle image densities. Exp Fluids 57(5), 70.

Schanz, D., Novara, M., Schröder, A. (2021). Shake-The-Box particle tracking with variable time-steps in flows with high velocity range (VT-STB). 14th Int. Symp. on PIV (ISPIV 2021), Chicago, USA (online).

Shyy, W., Aono, H., Chimakurthi, S.K., Trizila, P., Kang, C.-K., Cesnik, C.E.S., Liu, H. (2010). Recent progress in flapping wing aerodynamics and aeroelasticity, Progress in Aerospace Sciences 46: 284–327.

Wieneke, B. (2007). Volume self-calibration for 3D particle image velocimetry. Exp Fluids 45:549–556.

Wieneke,B. (2013) Iterative reconstruction of volumetric particle distribution. Meas Sci Technol 24:024008

Wolf, T., Konrath, R. (2015). Avian wing geometry and kinematics of a free-flying barn owl in flapping flight. Exp Fluids 56(28).